CHEMISTRY
AN ASIAN JOURNAL
www.chemasianj.org

Accepted Article

Title: Effect of Ligand Fields on the Reactivity of O2-Activating Iron(II)-Benzilate Complexes of Neutral N5 Donor Ligands

Authors: Shrabanti Bhattacharya, Reena Singh, and Tapan Kanti Paine

To be cited as: *Chem. Asian J.* 10.1002/asia.202000142

Link to VoR: http://dx.doi.org/10.1002/asia.202000142

A Journal of
ACES Asian Chemical Editorial Society

A sister journal of Angewandte Chemie and Chemistry – A European Journal

WILEY-VCH

10.1002/asia.202000142

WILEY-VCH

Effect of Ligand Fields on the Reactivity of O_2-Activating Iron(II)-Benzilate Complexes of Neutral N5 Donor Ligands

Shrabanti Bhattacharya,[a] Reena Singh*,[a] and Tapan Kanti Paine*,[a]

Dedicated to Professor Goutam Kumar Lahiri on his 60th Birthday

[a] Dr. S. Bhattacharya, Dr. R. Singh and Prof. T. K. Paine

School of Chemical Sciences, Indian Association for the Cultivation of Science, 2A&2B Raja S. C. Mullick Road, Jadavpur, Kolkata-700032, India.
E-mail: ictkp@iacs.res.in

Supporting information for this article is given via a link at the end of the document.

Abstract: Three new iron(II)-benzilate complexes $[(N4Py)Fe^{II}(benzilate)]ClO_4$ (**1**), $[(N4Py^{Me2})Fe^{II}(benzilate)]ClO_4$ (**2**) and $[(N4Py^{Me4})Fe^{II}(benzilate)]ClO_4$ (**3**) of neutral pentadentate nitrogen donor ligands have been isolated and characterized to study their dioxygen reactivity. Single crystal X-ray structures reveal a mononuclear six-coordinate iron(II) centre in each case, where benzilate binds to the iron center in monodentate mode via one carboxylate oxygen. Introduction of methyl groups in the 6-positions of the pyridine rings makes the $N4Py^{Me2}$ and $N4Py^{Me4}$ ligands weaker field compared to the parent N4Py ligand. All the complexes (**1-3**) react with dioxygen to decarboxylate the coordinated benzilate to benzophenone quantitatively. The decarboxylation takes lesser time for the complex of more sterically hindered ligand and follows the order **3**>**2**>**1**. The complexes display oxygen atom transfer reactivity to thioanisole and also exhibit hydrogen atom transfer reactions with substrates containing weak C-H bonds. Based on interception studies with external substrates, labelling experiment and Hammett analysis, a nucleophilic iron(II)-hydroperoxo species is proposed to form upon two-electron reductive activation of dioxygen by each iron(II)-benzilate complex. The nucleophilic oxidants are converted to the corresponding electrophilic iron(IV)-oxo oxidant upon treatment with a protic acid. The high-spin iron(II)-benzilate complex with the weakest ligand field results in the formation of a more reactive iron-oxygen oxidant.

Introduction

Dioxygen activating mononuclear nonheme iron enzymes perform a wide range of bio-transformation reactions.[1] Parallel to their versatile reactivity, the active sites of these enzymes exhibit a rich structural diversity.[2] In the dioxygen activation process by these enzymes, additional reducing equivalents are supplied either by cofactors or by substrates. In some cases, electrons are supplied by electron transfer proteins.[1b, 3] The cofactors/substrates bind to the active site iron center to overcome the low one-electron redox potential of dioxygen. Subsequent to dioxygen reduction at the iron center, different iron-oxygen intermediates are generated depending upon the structure and function of the enzymes.[1d] Along with the active site geometry, the spin state of iron center plays important roles in directing the reaction pathway. For example, a low-spin iron(III)-hydroperoxo species has been observed in the catalytic cycle of activated bleomycin (ABLM) enzyme.[4] While the active species in heme oxygenases has been characterized as a low-spin iron(IV)-oxoporphrin radical cation,[5] most of the nonheme oxygenases employ high-valent iron-oxo species in high-spin states.[6] A high-spin iron(IV)-oxo intermediate has been trapped and characterized in the catalytic cycle of taurine dioxygenase (TauD).[7] Subsequently, similar intermediates have been observed in other nonheme enzymes such as prolyl hydroxylase, tyrosine hydroxylases and in halogenases.[6, 8] An iron(III)-hydroperoxide intermediate has been crystallographically characterized in the *cis*-dihydroxylation of aromatic compounds catalyzed by Rieske dioxygenase.[9]

Functional modeling of enzymatic reactions provide useful mechanistic information about the catalytic cycle. As in enzymatic systems, synthetic high-spin iron(II) complexes are more reactive toward dioxygen than the corresponding low-spin complexes. A number of low-spin iron(II) complexes of nitrogen rich polydentate ligands, which are otherwise unreactive, have been shown to activate dioxygen in the presence of electron and proton source by tuning the ligand field through use of appropriate solvent.[10] Coordination of solvent molecules to iron center regulates the iron(II)/iron(III) redox potential facilitating the activation of O_2. Spin states of the iron centre have been demonstrated to modulate the strength of Fe–O and O–O bonds, and their cleavage in nonheme Fe-OOR/H species.[11] The spin-state effect is also manifested in the hydrogen atom transfer (HAT) and oxygen atom transfer (OAT) reactivity of synthetic iron(IV)-oxo complexes.[12] It has been demonstrated that increasing the population in high-spin state increases the reactivity.[13] This can be achieved by decreasing the energy gap between the low-spin and high-spin state through decrease in ligand field strength. In synthetic complexes, polydentate nitrogen ligands are extensively used and their ligand fields are tunable by appropriate substitution on the ligand backbone.[14] Methyl substitution on one of the pyridine rings of tris(2-pyridylmethyl)amine (TPA) has been reported to change the spin state of the resulting iron(II) complexes.[14e] The steric hindrance of the 6-Me substituents is manifested in the longer metal-ligand bonds and weaker ligand field. The effect of 6-Me substituents on the pyridine rings of the pentadentate N4Py scaffold in weakening the ligand field strength of the bis(6-methylpyridin-2-yl)-*N*,*N*-bis((pyridin-2-yl)methyl)methanamine ($N4Py^{Me2}$) ligand in the equatorial plane has been reported recently.[15]

We have been investigating the reductive activation of dioxygen by nonheme iron(II)-α-hydroxy acid complexes of ligands of varying denticity and their oxidizing ability in O_2-dependent oxidation reactions. In that direction, we have shown that iron-

coordinated benzilate acted as two-electron reductant and the reduced oxygen species on the iron center exhibited versatile reactivity.[16] The iron(II)-benzilate complexes of facial tridentate ligands displayed better reactivity in substrate oxidation compared to those of tetradentate ligands. Moreover, the geometry and topology of tetradentate ligands have been shown to play important roles in the oxygenation of substrates by O_2-derived iron-oxygen oxidants.[16] With an objective to understand the effect of methyl substitution on the pyridine rings of N4Py backbone and the resulting ligand field strengths on the oxidizing ability of the corresponding iron(II)-benzilate complexes, we have explored the dioxygen reactivity of three complexes, $[(N4Py)Fe^{II}(benzilate)]^+$ (**1**), $[(N4Py^{Me2})Fe^{II}(benzilate)]^+$ (**2**) and $[(N4Py^{Me4})Fe^{II}(benzilate)]^+$ (**3**) ($N4Py^{Me4}$ = bis(6-methylpyridin-2-yl)-*N*,*N*-bis((6-methylpyridin-2-yl)methyl)methanamine (Chart 1). With increasing number of methyl substitution on the pyridine rings of N4Py, the ligand field becomes weaker and the resulting iron-oxygen species becomes a stronger oxidant. The characterization, dioxygen reactivity of the iron(II)-benzilate complexes and the ligand field effect on O_2-dependent oxidation of substrates are presented in this work.

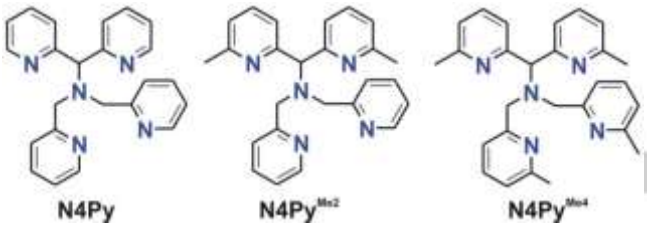

Chart 1. Ligands used in this work.

Results and Discussion

Synthesis and characterization

The N4Py ligand was synthesized using the procedure reported in the literature.[17] The ligands, $N4Py^{Me2}$ and $N4Py^{Me4}$, were prepared by the reductive amination of bis(6-methylpyridin-2-yl)methanamine[18] with pyridine-2-carboxaldehyde and 6-methylpyridine-2-carboxaldehyde, respectively, in dichloromethane. Reactions of equimolar amounts of iron(II) perchlorate, benzilic acid, triethylamine and the respective N5 ligand in methanol afforded bright yellow iron(II)-benzilate complexes (**1-3**) in good yields (Experimental Section). The iron(II)-acetonitrile complex $[Fe^{II}(N4Py^{Me4})(CH_3CN)(H_2O)]^{2+}$ (**4**) was prepared by mixing the ligand and iron(II) perchlorate hydrate in acetonitrile.

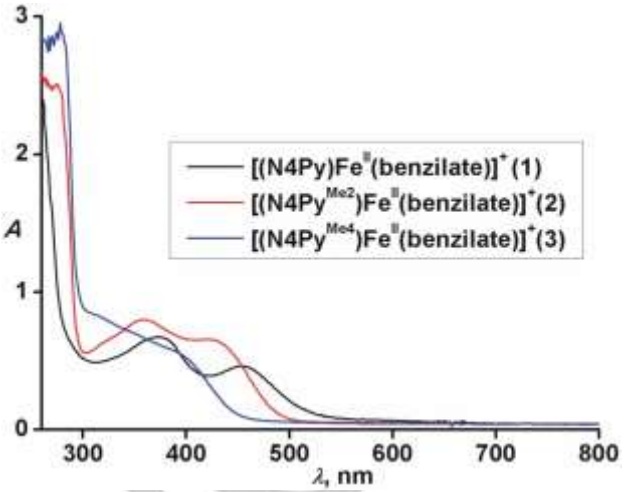

Figure 1. Optical spectra of iron(II)-benzilate complexes (**1**-**3**) under nitrogen atmosphere in acetonitrile (0.5 mM) at 298 K.

The optical spectra of the complexes in acetonitrile display bands in the region between 320 and 460 nm attributable to the ligand-centric and metal to ligand charge-transfer transitions, respectively (Figure 1). The band positions for **2** and **3** are blue shifted with the maximum shift observed for complex **3**. All the complexes exhibit broad and paramagnetically shifted proton resonances in between -25 and 55 ppm suggestive of the high-spin state of the complexes in solution (Figure S1, Supporting Information, SI). The room-temperature magnetic moment values between 5.1 μ_B and 5.2 μ_B further confirm the high-spin nature of the complexes.

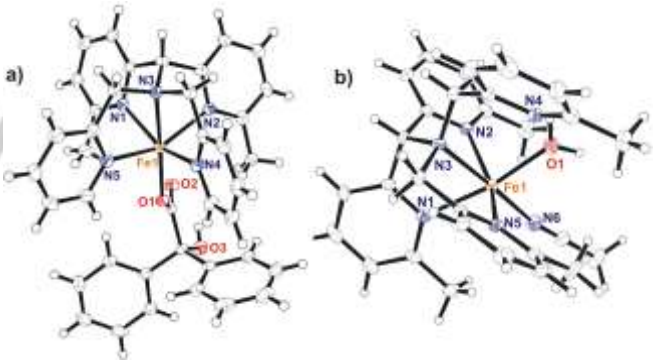

Figure 2. ORTEP diagrams of the cationic complexes (a) $[(N4Py^{Me2})Fe^{II}(benzilate)]^+$ (**2**) and (b) $[(N4Py^{Me4})Fe^{II}(CH_3CN)(H_2O)]^{2+}$ (**4**) with thermal ellipsoids at 30% probability.

The complexes were further characterized by single crystal X-ray diffraction. Complexes **1** and **2** crystallize in monoclinic system with the *P2(1)/c* space group, whereas complex **3** crystallizes in the monoclinic *P2(1)/n* space group (Table S1). In all the complexes, the coordination environment around the iron center is distorted octahedral, and in each case, the iron center is ligated by five nitrogen donors from the supporting ligand (Figures 2 and S2). The sixth coordination site is occupied by one carboxylate oxygen of the monoanionic benzilate. In each complex, the amine nitrogen (N3) and the carboxylate oxygen (O1) occupy the axial positions and the four pyridine nitrogens

constitute the equatorial plane. The two methyl groups on the pyridine donor of the ligand in complex **2** engender an asymmetric ligand field in the equatorial plane thereby causing more deviation in the axial N3-Fe-O1 angle from 180°. To adjust this deviation, the Fe1-N3 bond in complex **2** is slightly elongated compared to that in **1** and **3**. The average Fe-N bond distances are observed in the range between 2.18 Å and 2.26 Å, typical of high-spin iron(II) complexes (Table 1).[19] Upon introduction of two and four methyl substituents on the pyridine rings, the Fe-N_{Py} bonds are elongated in the equatorial plane to avoid steric interactions. The ligand field strength thus follows the order N4Py> $N4Py^{Me2}$> $N4Py^{Me4}$.

Table 1. Selected bond length (Å) and angles (°) of complexes **1**, **2**, **3** and **4**.

Bond distance/ bond angle	**1**	**2**	**3**	**4**
Fe1-O1^{benzilate}	1.972(8)	1.9970(19)	2.014(3)	-
Fe1-O1^{H2O}	-	-	-	2.053(5)
Fe1-N6^{MeCN}	-	-	-	2.122(7)
Fe1-N5	2.138(11)	2.170(2)	2.251(4)	2.266(5)
Fe1-N4	2.190(9)	2.190(2)	2.268(3)	-
Fe1-N2	2.172(9)	2.226(2)	2.251(4)	2.293(5)
Fe1-N3	2.232(9)	2.250(2)	2.212(3)	2.220(5)
Fe1-N1	2.198(11)	2.266(2)	2.293(3)	2.209(6)
O1-Fe1-N5	105.1(7)	94.30(8)	111.23(13)	-
O1-Fe1-N4	94.0(4)	94.31(8)	110.17(12)	-
N5-Fe1-N4	85.8(3)	87.75(9)	84.63(13)	-
O1-Fe1-N2	100.8(4)	113.00(8)	98.13(12)	-
N5-Fe1-N2	153.9(7)	152.62(9)	150.61(14)	152.8(2)
N4-Fe1-N2	88.5(3)	88.13(8)	86.70(13)	-
O1-Fe1-N3	170.8(4)	167.95(8)	168.70(12)	-
N5-Fe1-N3	77.2(6)	77.58(9)	77.14(13)	76.11(19)
N4-Fe1-N3	77.2(4)	76.66(9)	77.51(13)	-
N2-Fe1-N3	76.7(4)	75.12(8)	73.57(13)	76.83(19)
O1-Fe1-N1	114.9(5)	114.44(8)	98.60(11)	-
N5-Fe1-N1	88.9(4)	86.17(9)	86.41(12)	94.9(2)
N4-Fe1-N1	150.9(6)	150.96(9)	151.18(14)	-
N2-Fe1-N1	83.8(4)	84.40(8)	87.82(12)	94.9(2)
N3-Fe1-N1	73.8(5)	74.31(8)	84.63(13)	77.1(2)

A related iron(II) complex **4** was structurally characterized for comparison with the iron(II)-benzilate complex **3**. The iron center in **4** is coordinated by four nitrogen donors from the $N4Py^{Me4}$ ligand and the remaining sites are occupied by one acetonitrile and one water molecule giving rise to a distorted octahedral coordination geometry. The steric bulk exerted by the 6-Me substituents restrains coordination of one of the pyridyl nitrogen atoms (N4). In the structure, the axial positions are occupied by the amine nitrogen (N3) and the nitrogen atom (N6) of the acetonitrile molecule with the N3-Fe1-N6 angle being 175.9(2)° (Table 1). The three pyridine nitrogens (N1, N2, N5) from ligand and the oxygen O1 from the water molecule constitute the equatorial plane. The Fe-N and Fe-O bond distances are within the range 2.12-2.29 Å and 2.05 Å, respectively, similar to those observed in the high-spin iron complex **3** of the ligand (Table 1).

Dioxygen reactivity of iron(II)-benzilate complexes

The iron(II)-benzilate complexes (**1-3**) react with dioxygen in acetonitrile at ambient conditions to display oxidative decarboxylation of benzilic acid to benzophenone. While complex **1** does not show any appreciable change in the optical spectra even after 24 h, the intensities of the CT bands (at 350 nm and 450 nm for complex **2**, and at 370 nm for complex **3**) increase slowly generating broad featureless spectra (Figure 3). Interestingly, the time required for complete decarboxylation varies with the number of methyl substituents on the ligand backbone. Complex **1** takes nearly 24 h for decarboxylation, whereas complexes **2** and **3** quantitatively decarboxylate in 6 h and 2 h, respectively. Thus, the rate of decarboxylation has clear dependence on the ligand; sterically hindered the ligand faster is the decarboxylation. The oxidized solutions of complexes **2** and **3** at 77 K are found to be EPR silent, whereas for complex **1**, a signal at g = 4.2 is observed in the X-band EPR spectrum (77 K) after the reaction with O_2 indicating the presence of a high spin iron(III) species as the end product (Figure S3). Time-dependent ^{1}H NMR spectra of the complexes during the reaction with dioxygen show gradual changes with the disappearance of some resonance signals yielding broad signals at the end of the reactions (Figure S4). On the contrary, the NMR spectra of the oxidized complexes from **2** and **3** bear resemblance to the precursor iron(II) complexes. The ^{1}H NMR spectrum of the organic product derived from benzilate establishes quantitative decarboxylation of benzilate to benzophenone in each case (Figure S5).

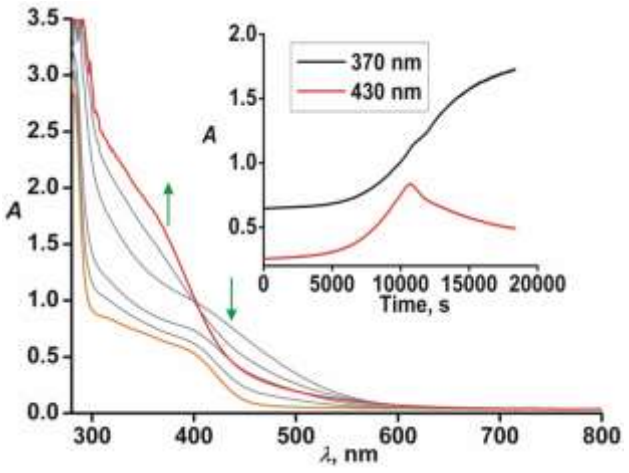

Figure 3. Optical spectral changes during the reaction of **3** (0.5 mM in acetonitrile) with dioxygen at 295 K.

Since no iron-oxygen species could be trapped even at low temperature for direct characterization, indirect probes were used to intercept the oxidant formed upon oxidative decarboxylation of the iron(II)-benzilate complexes (Table 2). When thioanisole (20 equiv.) is separately added to the acetonitrile solutions of the complexes **1**-**3** in the presence of O_2, thioanisole oxide is formed as the sole product (Figure S6 and Table 2). When the equiv of thisoanisole is decreased (2 equiv.), methyl phenyl sulfone is detected along with sulfoxide (Figure S7 and Table 2). The yield of the product is however found to decrease systematically from **3** to **1** (Table 2). Other substrates such as 9,10-dihydroanthracene, fluorene, toluene and cyclohexene are converted to their oxidized forms (Table 2). Alkenes such as styrene, 1-octene, cyclooctene and cyclohexane are, however, unreactive in the reaction conditions. When *p*-bromobenzaldehyde (or benzaldehyde) is used as intercepting agent, *p*-bromobenzoic acid (or benzoic acid) is formed as the sole products (Table 2 and Figure S8).

Table 2. Oxidation of substrates with oxygen by the iron(II)-benzilate complexes.

Substrates (equiv.)	Products	**1** (%)	**2** (%)	**3** (%)
Thioanisole (20)	Thioanisole oxide	12	55	84
Thioanisole (2)	Thioanisole oxide + Methyl phenyl sulfone	0+3	5+8	9+16
4-Bromo-benzaldehyde (20)	4-Bromobenzoic acid	5	12	20
Benzaldehyde (20)	Benzoic acid	3	10	15
9,10-Dihydro-anthracene (5)	Anthracene + Aanthraquinone	18+3	36+2	50+5
Fluorene (5)	Fluorenone	15	30	45
Toluene (100)	Benzaldehyde	-	6	15
Cyclohexene (100)	2-Cyclohexen-1-ol + 2-Cyclohexen-1-one	-	12+5	21+10

The sulfoxidation reaction by **3** in the presence of $H_2{}^{18}O$ does not incorporate any labeled oxygen into the product. However, the GC-mass spectra of the organic products formed in the reaction with thioanisole and $^{18}O_2$ confirm the incorporation of labeled oxygen into the oxygenated products (Figure S9). It is to be noted that the decarboxylation product (benzophenone) does not contain any labeled oxygen. Based on sulfone formation at low sulfide concentrations, a nucleophilic iron-oxygen oxidant is proposed as the active oxidant.[16, 20] The labeling experiment with $^{18}O_2$ and benzaldehyde suggests the incorporation of one oxygen atom into benzoic acid (Figure S10).

For Hammett analysis, competitive oxidations were carried out with 1:1 mixtures of thioanisole and different *para*-substituted thioanisoles (*p*-$XC_6H_4SCH_3$ where X = NO_2, Cl, H, Me, OMe). The ρ values of +0.63 and +0.81 for **2** and **3,** respectively, are obtained from the plots of the relative rates (k_{rel}) versus σ_p (Figure 4). Hammett analysis was not performed for **1** due to the low yield of thioanisole oxide in that case. Product distribution and Hammett analyses indicate that the oxidant from **2** is relatively weaker nucleophile than that from **3**.

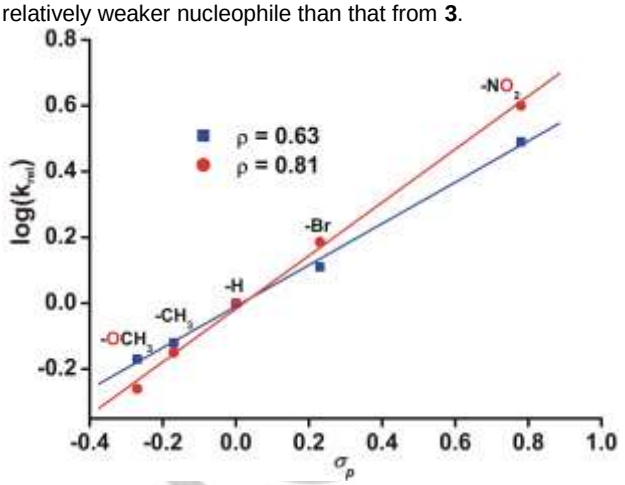

Figure 4. Hammett plot of log k_{rel} versus σ_p for *p*-$XC_6H_4SCH_3$ in the oxidation by complex **2** (blue square) and complex **3** (red circles). The k_{rel} value was calculated by dividing the concentration of the product from *p*-$XC_6H_4SCH_3$ by the concentration of the product from $C_6H_5SCH_3$.

Based on the interception results, labelling experiment and Hammett analysis, a nucleophilic iron(II)-hydroperoxo species is proposed to form upon two-electron reductive activation of dioxygen in the oxidative decarboxylation of benzilic acid to benzophenone. Similar intermediates have been proposed in the decarboxylation of iron(II)-α-hydroxy acid complexes of tridentate and tetradentate ligands.[16, 20b, 21]

Dioxygen reactivity of the iron(II)-benzilate complexes in the presence of protic acid

The effect of protic acid on the reactivity of iron(II)-benzilate complexes toward different organic substrates was investigated. While the dioxygen-derived oxidant from iron(II)-benzilate complexes (**1-3**) are unreactive towards alkenes, the substrates are converted to the corresponding epoxides by the oxidants generated in the presence of pyridinium perchlorate (1 equiv.) (Table 3). Cyclooctene is converted to cyclooctene oxide (Figure S11) in 48% and 64% yields by **2** and **3**, respectively. When 1-octene is used, 1,2-epoxyoctane (Figure S12) is formed. The oxidant also converts *cis*-2-heptene to 2-butyl-3-methyl oxirane (Figure S13) in 62% yield for **2** and 88% for **3**. When styrene is used, 2-phenyl oxirane is formed as the only product in 12% and 22% conversion by complex **2** and **3**, respectively (Figure S14a). The labeling experiment for styrene oxidation with $^{16}O_2$ and $H_2{}^{18}O$ by **3** reveals 10% incorporation of labeled oxygen atom into 2-phenyl oxirane (Figure S14b). Thus the oxidant formed in the presence of protic acid can exchange its oxygen atom with water. When cyclohexene is used as a substrate, the corresponding epoxide is formed in small amount. In the reaction, allylic oxidation products are observed as major product (Figure S15).

Table 3. Oxidation of substrates by complexes **2** and **3** with dioxygen in the presence of pyridinium perchlorate (1 equiv.).

Substrate (equiv)	Products	**2**	**3**	[($Tp^{Ph,Me}$)Fe^{II}(benzilate)] [22]	[(Tp^{Ph2})Fe^{II}(benzilate)] [22]
Thioanisole (20)	$PhSOCH_3$	53±2	85±1	97±1	90
Cyclooctene (100)	Cyclooctene oxide	48±2	64±1	58±1	70
Cyclohexene (100)	Cyclohexene oxide 2-Cyclohexen-1-ol 2-Cyclohexen-1-one 7-oxa-bicyclo[4.1.0]heptan-2-one	5 26 7 2	10 42 5 9	31±2 20 ±2 5±1 0	35 22 5 -
1-Octene (100)	1,2-Epoxyoctane	0	6±1	56±2	67
Styrene (100)	2-Phenyloxirane	12±1	22±2	-	75
cis-2-Heptene (100)	2-Butyl-3-methyl oxirane	62±2	88±1	-	-
Cyclohexane (100)	Cyclohexanol Cyclohexanone	26±1 10±2	42±2 15±2	58±3 6±1	45 8
Adamantane (5)	1-Adamantanol 2-Adamantanol 2-Adamantanone	-	34±2 0 4±2	65±4 <2 <4	47 18 0

In the oxidation of cyclohexane by complexes **2** and **3** in the presence of protic acid, cyclohexanol and cyclohexanone are formed exhibiting A/K ratio of 2.6 and 2.8, respectively (Figure S16). Notably, no oxidized product is detected from cyclohexane in the reaction with complex **1** alone. However, complex **3** is found to oxidize adamantane with a C3/C2 normalized selectivity of 26 (Figure S17, Table 3). Recently, similar C3/C2 selectivity has been reported in oxidation of adamantane with *m*-CPBA or oxone by the iron(II) complex [Fe^{II}($N4Py^{Me2}$)(CH_3CN)]($OTf)_2$ complex.[15] To rule out the involvement of a free radical mechanism, substrate oxidations were carried out in the presence of radical scavengers such as *tert*-butanol and 1,4-benzoquinone. Although the cyclohexanol/cyclohexanone ratio does not change in cyclohexane oxidation but the yield of 7-oxa-bicyclo[4.1.0]heptan-2-one formed from cyclohexene is completely reduced. This result suggests the generation of over-oxidized product from cyclohexene via radical pathway is inhibited by radical scavenger. A kinetic isotope effect (KIE) value of 3.8 in the competitive oxidation of a mixture of cyclohexane and cyclohexane-d_{12} by complex **3** also supports the involvement of a metal-based oxidation. These results indicate the generation of an electrophilic oxidant which could carry out epoxidation of alkenes and the C-H bond oxidation of cyclohexane (Table 3). The fact that the N4Py and $N4Py^{Me2}$ ligands can support the iron(IV)-oxo unit [15] and the results from mechanistic and interception studies together indicate that iron(IV)-oxo species is generated in situ in the dioxygen-dependent decarboxylation of the iron-benzilate complexes. As reported for the Tp^{Ph2} system,[23] an iron(IV)-oxo species is proposed as the active oxidant from the respective iron(II)-benzilate complexes that performs the epoxidation reactions in the presence of a protic acid. Importantly, the oxidative decarboxylation is not affected in the presence of proton donor. The reaction of complex **3** with thioanisole (20 equiv.) and pyridinium perchlorate (1 equiv.) afforded thioanisole oxide as the sole product (Figure S18). Hammett analyses from competitive oxidations of equimolar amounts of *para*-substituted thioanisoles and thioanisole by complex **3** in the presence of protic acid and dioxygen reveal a negative ρ value of -0.90 (±0.08) indicating that an electrophilic oxidant is responsible for sulfide oxidation (Figure 5).

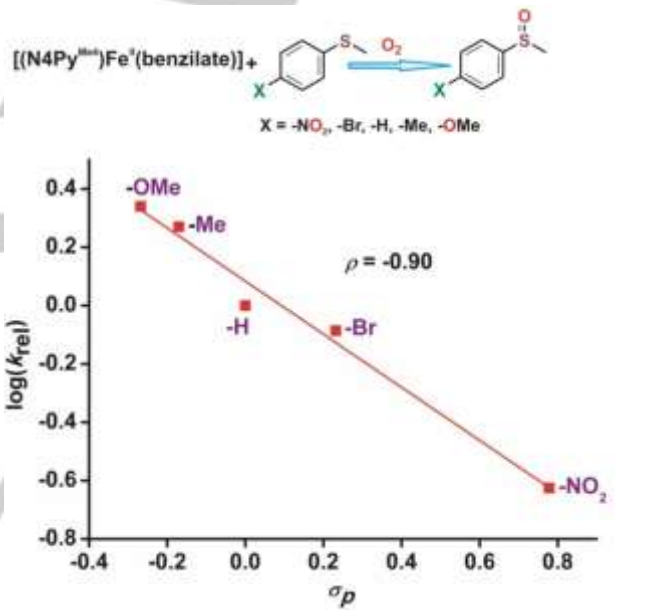

Figure 5. Hammett plot for the oxidation of *p*-X-C_6H_4SMe by **3** with $PyNHClO_4$ (1 equiv).

The iron(II)-benzilate complexes supported by tris(pyrazolyl)borate ligands have been reported to oxygenate alkenes to *cis*-diols with the incorporation of both the oxygen atoms of dioxygen. Further mechanistic studies suggested the involvement of a nucleophilic iron-oxygen oxidant in the *cis*-dihydroxylation reactions. However, the nucleophilic oxidant changed its philicty in the presence of a Lewis acid[21] and protic acid.[23] Lewis acid or protic acid cleaves the O-O bond of the putative iron(II)-hydroperoxide heterolytically to generate an electrophilic iron(IV)-oxo-hydroxo and iron(IV)-oxo-aquo species, respectively. Furthermore, the electrophilic oxidants oxygenated the strong C-H bonds of aliphatic substrates. In the absence of any substrate, the oxidants intramolecularly hydroxylated one of the phenyl rings of the Tp^{Ph2} ligand. The intraligand hydroxylation was inhibited by replacing the 5-phenyl groups on the pyrazole rings of the ligand by methyl groups.[22] The iron(II)-

benzilate complex of the $Tp^{Ph,Me}$ ligand displayed enhanced reactivity under stoichiomteric conditions. Furthermore, the complex exhibited catalytic oxygenations and the catalytic activity was improved upon addition of a Lewis acid. The iron(II)-benzilate complexes of tetradentate nitrogen ligands also displayed diverse reactivity toward alkenes depending upon ligand topology. It was proposed that the side-on-bound iron(II)-hydroperoxides were able to *cis*-dihydroxylate the C=C bonds of olefins, whereas the end-on iron(II)-hydroperoxides was unable to oxygenate the alkenes.[16]

The iron(II)-benzilate complexes discussed in this work display moderate reactivity in oxygen atom transfer (OAT) and in hydrogen atom transfer (HAT) reactions on substrates with weak C-H bonds. The iron(II)-benzilate complexes of ligands with 6-methyl substitution (**2** and **3**) show better reactivity compared to that of **1**. Of note, complexes **2** and **3** exhibit higher reactivity in OAT transfer reaction in comparison to that of the iron(II) complexes of tetradentate systems.[16] In fact, the OAT ability of the oxidants from **2** and **3** closely match to that of the complexes of tridentate ligand (Table 4). The increased reactivity of the complexes over the reported iron(II) complexes of tetradentate ligands can be attributed to the significant steric constraint of the ligands that prevent dimerization and other unwanted bimolecular side reactions.

Table 4. Comparison of the reactivity of iron(II)-benzilate complexes $[(L)Fe^{II}(benzilate)]^+$ of different ligands.

L	Reaction time	Yields (%) of the products from substrates			
		$PhSOCH_3$ + $PhSO_2CH_3$ from thio-anisole	Octane-1,2-diol from 1-octene	*cis*-Cyclo-octane-1,2-diol from cyclo-octene	Anthra-cene from 9,10-Dihydro anthra-cene
Tp^{Ph2} [22]	15 min	84 + 7	85	80	-
$Tp^{Ph,Me}$ [22]	45 min	93+ 4	92	86	-
TPA[16]	2 h	17	-	-	22
6-Me_3-TPA[16]	4 h	67	12	16	26
iso-BPMEN[16]	1.5 h	20	-	-	21
6-Me_2-*iso*-BPMEN[16]	2 h	37 + 5	-	-	28
BPMEN[16]	4.5 h	21	<5	<5	24
6-Me_2-BPMEN[16]	5.5 h	61	21	12	34
TBimA[16]	2.2 h	25	-	-	38
N4Py	20 h	12	-	-	18
$N4Py^{Me2}$	6 h	55	-	-	36
$N4Py^{Me4}$	2 h	84	-	-	50

On the basis of the results discussed above, a mechanism similar to that proposed for other reported iron(II)-benzilate complexes is put forward.[16] From the crystal structure of **3**, it is clear that the average iron-$N_{pyridine}$ distance is longer than those in other complexes. Although complex **4** is not reactive toward dioxygen, its crystal structure (Figure 2b) provides information about a possible pathway of the reaction between iron(II)-benzilate complex **3** and O_2 . One of the hemilabile pyridine arms may get de-coordinated to avoid steric congestion, which in turn facilitates dioxygen activation at the iron(II) center in **3**. The de-coordination step is most facile in **3** among the three complexes and least in complex **1**. Upon binding of dioxygen and subsequent reduction by the co-ligand benzilate, an end-on bound nucleophilic iron(II)-hydroperoxo (**I**) intermediate is formed. Transfer of one of the oxygen atoms to external substrates results in iron(II)-hydroxide species as the final species. The UV-vis spectra of the oxidized solutions after the reaction with dioxygen show featureless broad spectra. Furthermore, an ion peak corresponding to $[LFe^{II}\text{-}OH(H_2O)]^{2+}$ is observed at *m/z* 486 for the oxidized complex of **2** in the ESI-mass spectrometry (Figure S19). No such species is detected for the oxidized solution of complex **1**.

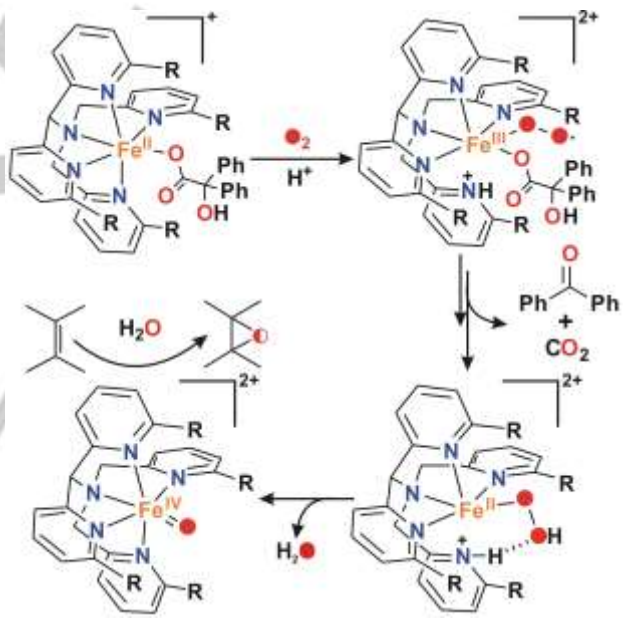

Scheme 1. Mechanistic proposal for the formation of iron-oxygen oxidants in the oxidative decarboxylation of α-hydroxy acids in the presence of a protic acid.

In the presence of protic acid, the de-coordinated pyridine ring likely gets protonated (Scheme 1). The protonated pyridine upon interaction with the hydroperoxide moiety may facilitate the heterolytic O-O bond cleavage with the formation of iron(IV)-oxo species. The high-valent iron-oxo species can exchange its oxygen atom with water and performs epoxidation of alkenes and C-H bond hydroxylation of aliphatic substrates including those of cyclohexane.

Conclusion

Three new iron(II)-benzilate complexes supported by pentadentate N4Py-derived ligands were isolated and structurally characterized. The ability of the complexes in carrying out O_2-dependent oxidations particularly oxygen atom transfer (OAT) and hydrogen atoms transfer (HAT) was investigated. The complexes activate dioxygen and display quantitative decarboxylation of benzilic acid to benzophenone. Enhanced reactivity of the complexes in sulfide oxidation is observed compared to the related complexes of tetradentate ligands. Moreover, the complexes exhibit HAT reactions on substrates with weak C-H bonds. Based on the interception and labelling experiments, a putative iron(II)-hydroperoxo intermediate is proposed as the active oxidant. The presence of a protic acid changes the philicity of the iron-oxygen intermediate from a nucleophilic iron(II)-hydroperoxo to an electrophilic iron(IV)-oxo species. Effect of substitution on ligand backbone in directing the reactivity of iron(II)-benzilate complexes is demonstrated. The reactivity trend of the iron(II)-benzilate complexes discussed in this work implicate the role of ligand field in performing dioxygen-dependent oxidation reactions and that weak-field ligands are more appropriate to promote O_2-based reactivity using two-electron sacrificial reductants. Further studies to trap the proposed iron-oxygen intermediates from iron(II)-benzilate complexes of polydentate ligands are presently being pursued in our laboratory.

Experimental Section

Materials and Methods. All chemicals and reagents were obtained from commercial sources and were used without further purification unless otherwise noted. Solvents were distilled and dried before use. Preparation and handling of air-sensitive materials were carried out under an inert atmosphere in a glove box. Fourier transform infrared spectroscopy on KBr pellets was performed on a Shimadzu FT-IR 8400S instrument. Elemental analyses were performed on a Perkin Elmer 2400 series II CHN analyzer. Electro-spray ionization (ESI) mass spectra were recorded with a Waters QTOF Micro YA263 instrument. Solution electronic spectra (single and time-dependent) were measured on an Agilent 8453 diode array spectrophotometer. All room temperature NMR spectra were collected on a Bruker Avance 500 MHz spectrometer. X-band EPR measurements were performed on a JEOL JES-FA 200 instrument. GC-MS measurements were carried out with a Perkin Elmer Clarus 600 using Elite 5 MS (30m x 0.25mm x 0.25µm) column with a maximum temperature of 300°C. Labeling experiments were carried out with $^{18}O_2$ gas (99 atom %) or $H_2{}^{18}O$ (98 atom %) purchased from Icon Services Inc., USA.

Ligand Synthesis. The N4Py and N4Py^{Me2} ligands were synthesized according to the procedure reported in the literature.[53,41] Bis(6-methylpyridin-2-yl)methanone, bis(6-methylpyridin-2-yl)methanoneoxime, and bis(6-methylpyridin-2-yl)methanaminewere prepared according to the procedures reported in literature.[18] *Although no problem was encountered during the synthesis of these complexes, perchlorate salts are potentially explosive and should be handled with care!*[24]

Synthesis of N4Py^{Me4}. To a mixture of bis(6-methylpyridin-2-yl)methanamine (0.500 g, 2.35 mmol) and sodium triacetoxyborohydride (3.44 g, 16.2 mmol) in dichloromethane (50 mL) was added 6-methyl-pyridine-2-carboxaldehyde (0.594 g, 4.9 mmol). The mixture was allowed to stir for 48 h at ambient temperature. Subsequently, a saturated aqueous sodium hydrogen carbonate solution was added followed by stirring for an additional 1 h. The organic product was then extracted with dichloromethane (3 x 50 mL). The combined organic extracts were dried over Na_2SO_4 and evaporated to dryness to yield a pale yellow oil. Yield: 0.45 g (48%). ^{1}H NMR (500 MHz, DMSO-d_6, 298 K): δ(ppm) 7.40-7.50 (m, 4H), 7.05 (dd, 4H), 6.99 (dd, 2H), 6.87 (dd, 2H), 5.18 (s, 1H), 4.71 (s, 4H), 2.48 (s, 6H), 2.45 (s, 6H). ESI-MS (+ve ion mode, acetonitrile): *m/z* 424.1 (100%, $[M+H]^+$), 446.1 (40%, $[M+Na]^+$).

General Procedure for the Syntheses of Iron(II) Benzilate Complexes. Iron(II) perchlorate hydrate (0.36 g, 1 mmol) was added to a solution of the ligand (1 mmol) in methanol(5 mL). To the resulting solution was dropwise added an equimolar mixture of benzilic acid (0.23 g, 1 mmol) and triethylamine (240 µL, 1 mmol). The solution was then stirred at room temperature for 5 h to afford the microcrystalline yellow solid compounds **1**-**3**.

[(N4Py)Fe^{II}(benzilate)](ClO$_4$)$_2$ (1). Single crystals suitable for X-ray diffraction were obtained by diffusion of hexane into a solution of the complex in dichloromethane. Yield: 0.69 g (83%). Anal. Calcd for $C_{38}H_{34}Cl_3FeN_5O_7$ (834.90 g/mol): C, 54.67; H, 4.10; N, 8.39. Found: C, 54.61; H, 4.05; N, 8.31. IR (KBr, cm^{-1}): 3053 (m), 3038 (m), 3001 (m), 1638 (s), 1605 (s), 1576 (m), 1481 (s), 1443 (s), 1346 (m), 1157 (m), 1016 (m), 760 (m), 737 (s), 706 (s). UV−vis in CH_3CN (λ_{max}): 374 nm (ε = 1340 M^{-1} cm^{-1}), 450 nm (ε = 918 M^{-1} cm^{-1}). Magnetic moment μ_{eff} (298 K): 5.1 μ_B. ^{1}H NMR in $CDCl_3$ (500 MHz; δ (ppm)): 90.3 (Py-H$_\alpha$), 54.3 (CH_2Py), 48.3 (Py-H$_\beta$), 46.5 (Py-H$_{\beta'}$), 32.5 (Py-H$_\gamma$), 25.5 (NCH-Py-H$_\beta$, NCH-Py-H$_{\beta'}$), 22.8 (NCH-Py-H$_\gamma$), 9.4 (benzilate-o-H), 8.2 (benzilate-m-H), 7.3 (benzilate-p-H), 7.7 (NCH-Py-H$_\alpha$), 7.2 (N-CH).

[(N4Py^{Me2})Fe^{II}(benzilate)](ClO$_4$)$_2$ (2). Single crystals suitable for X-ray diffraction were obtained by diffusion of diethyl ether into a solution of the complex in acetonitrile. Yield: 0.61 g (78%). Anal. Calcd for $C_{39}H_{36}ClFeN_5O_7$ (778.03 g/mol): C, 60.21; H, 4.66; N, 9.00. Found: C, 59.31; H, 4.58; N, 8.89. IR (KBr, cm^{-1}): 3053 (m), 3038 (m), 3001 (m), 1638 (s), 1605 (s), 1576 (m), 1481 (s), 1443 (s), 1346 (m), 1157 (m), 1016 (m), 760 (m), 737 (s), 706 (s). UV−vis in CH_3CN (λ_{max}): 356 nm (ε = 1580 M^{-1} cm^{-1}), 433 nm (ε = 1260 M^{-1} cm^{-1}). Magnetic moment μ_{eff} (298 K): 5.2 μ_B. ^{1}H NMR in $CDCl_3$ (500 MHz; δ (ppm)): 87.8 (Py-H$_\alpha$), 51.0 (CH_2Py), 49.4 (Py-H$_\beta$), 46.1 (Py-H$_{\beta'}$), 38.5 (Py-H$_\gamma$), 28.2 (Me-Py-H$_\beta$, Me-Py-H$_{\beta'}$), 27.7 (Me-Py-H$_\gamma$), 9.4 (benzilate-o-H), 8.3 (benzilate-m-H), 7.4 (benzilate-p-H), 7.3 (N-CH), -15.2 (Me-Py-CH_3).

[(N4Py^{Me4})Fe^{II}(benzilate)](ClO$_4$)$_2$ (3). Single crystals suitable for X-ray diffraction were obtained by diffusion of diethyl ether into a solution of the complex in dichloromethane. Yield: 0.70 g (86%). Anal. Calcd for $C_{41}H_{40}ClFeN_5O_7$ (806.08 g/mol): C, 61.09; H, 5.00; N, 8.69. Found: C, 59.91; H, 4.88; N, 8.81. IR (KBr, cm^{-1}): 3053 (m), 3038 (m), 3001 (m), 1638 (s), 1605 (s), 1576 (m), 1481 (s), 1443 (s), 1346 (m), 1157 (m), 1016 (m), 760 (m), 737 (s), 706 (s). UV−vis in CH_3CN (λ_{max}): 380 nm (ε = 1320 M^{-1} cm^{-1}). Magnetic moment μ_{eff} (298 K): 5.2 μ_B. ^{1}H NMR in $CDCl_3$ (500 MHz; δ (ppm)): 54.9 (CH_2Py), 46.6 (Py-H$_\beta$), 44.7 (Py-H$_{\beta'}$), 22.2 (Py-H$_\gamma$), 16.8 (NCH-Py-H$_\beta$, NCH-Py-H$_{\beta'}$), 11.0 (NCH-Py-H$_\gamma$), 10.0(benzilate-o-H), 8.2 (benzilate-m-H), 7.3 (benzilate-p-H), -7.2 (N-CH), 3.1 (CH_2-Py-CH_3), -22.0 (NCH-Py-CH_3).

[Fe^{II}(N4Py^{Me4})(CH$_3$CN)(H$_2$O)](ClO$_4$)$_2$ (4). Iron(II) perchlorate hydrate (0.36 g, 1 mmol) and ligand (0.42 g, 1 mmol) were mixed together in acetonitrile (5 mL). The resulting solution was stirred at room temperature under N_2 atmosphere for 5 h. Single crystals suitable for X-ray diffraction were obtained by diffusion of diethyl ether into the acetonitrile solution of the complex. Yield: 0.64 g (86%). Anal. Calcd for $C_{29}H_{34}Cl_2FeN_6O_9$ (737.37 g/mol): C, 47.24; H, 4.65; N, 11.40. Found: C, 47.01; H, 4.63; N, 11.31. ESI-MS (+ve ion mode in CH_3CN): *m/z* 239.6 (100%) $[Fe(N4Py^{Me4})]^{2+}$.IR (KBr, cm^{-1}): 3053 (m), 3038 (m), 3001 (m), 1638 (s), 1605 (s), 1576 (m), 1481 (s), 1443 (s), 1346 (m), 1157 (m), 1016 (m), 760 (m), 737 (s), 706 (s). UV−vis in CH_3CN (λ_{max}): 376 nm (sh). Magnetic moment μ_{eff} (298 K): 5.2 μ_B. ^{1}H NMR (500 MHz in CD_3CN): δ(ppm) 82.4 (CH_2Py-Fe-coordinated), 61.1 (H_β-CH_2-Py-Fe-coordinated), 57.3 ($H_{\beta'}$-CH_2-Py-Fe-coordinated), 53.0 (H_γ-CH_2-Py-Fe-coordinated),

47.8 (CH_2-Py), 25.6 (CH_2-Py-H_β, CH_2-Py-$H_{\beta'}$), 18.4 (CH_2-Py-H_γ), 13.8 (NCH-Py-H_β, NCH-Py-$H_{\beta'}$), 8.4 (NCH-Py-H_γ), -5.0 (CH_3-CH_2-Py-Fe-coordinated), -6.3 (N-C*H*), -27.2 (CH_3-CH_2-Py), -40.8 (NCH-Py-CH_3).

Reaction of Iron(II)-Benzilate Complexes with O_2 and Analysis of Organic Products. For a stoichiometric reaction, solid complex (0.02 mmol) was dissolved in dry acetonitrile (15 mL) under nitrogen atmosphere. Pure O_2 was passed through the solution, and the mixture was stirred at room temperature, during which the initial light yellow solution slowly turned light orange. The solution was concentrated and the residue was treated with 2 M HCl (10 mL). The organic products were then extracted with diethyl ether (3 × 20 mL) and dried over anhydrous sodium sulfate. The organic layer was filtered and evaporated to dryness. The products were analyzed by ^{1}H NMR and GC-MS without further purification. Quantification of the products were done by using 1,3,5-trimethoxy benzene and naphthalene as internal standards for ^{1}H NMR and GC-MS, respectively.

Reactions of Iron(II) Complexes with Substrates. The iron(II) benzilate complex (0.02 mmol) were dissolved in dioxygen-saturated organic solvent under a nitrogen atmosphere. Substarte was added to the solution and was allowed to stir at room temperature for 2 h. After oxidation, the solvent was removed under reduced pressure and the iron complex was decomposed by addition of 3 M HCl solution (10 mL). The organic products were extracted by either diethyl ether or chloroform (3 × 15 mL), and the organic layer was dried over anhydrous sodium sulfate. After removal of the solvent, organic products were analyzed by GC-MS and ^{1}H NMR spectroscopy. For reactions with alkenes, the products were analyzed by GC-MS spectroscopy. Quantification of the organic products by NMR was done by comparing the peak area of four aromatic *ortho* protons (7.81 ppm) of benzophenone. For GC analyses, naphthalene was used as an internal standard and the products were identified by comparison of their GC retention times and GC-MS with those of authentic compounds. ^{1}H NMR Data: Benzophenone: δ 7.81 (d, 4H), 7.59 (t, 2H), 7.48 (t, 4H), 4- bromobenzoic acid: δ 7.95 (d, 2H), 7.65 (d, 2H). Methyl phenyl sulfone: δ 7.94 (d, 2H), 7.61 (m, 3H), 3.10 (s, 3H).

Control Experiments. For control experiments, iron(II) perchlorate was allowed to react with O_2 in the presence of external substrate. The reaction was carried out following the same procedure mentioned above except that iron(II) perchlorate hexahydrate (0.01 mmol) was used instead of iron(II) benzilate complex. No oxidized product derived from organic substrates was observed in any of the experiments. In a different set of control experiments, iron(II) perchlorate hexahydrate and monoanionic benzilate (benzilic acid in the presence of 1 equiv. of triethylamine) was used that resulted a trace amount (<5%) of benzophenone. However, substrate oxidation was not observed in the above reaction.

X-ray Crystallographic Data Collection, Refinement and Solution of the Structure. X-ray single-crystal data for the complexes were collected using Mo Kα (λ = 0.7107 Å) radiation on a SMART-APEX diffractometer equipped with CCD area detector. Details of the data collection and structure refinement are provided in (Table S1). Data collection, data reduction, structure solution and refinement were carried out using the software package of APEX II.[25] The structure was solved by intrinsic methods and subsequent Fourier analyses and refined by the full-matrix least-squares method basedon F^2 with all observed reflections.[26] The non-hydrogen atoms were treated anisotropically. The disordered carbon atoms were treated isotropically. CCDC 1960560, 1960559, 1960558, and 1960561 contain the supplementary crystallographic data for **1, 2, 3** and **4,** respectively. The data can be obtained free of charge from the Cambridge Crystallographic Data Centre via www.ccdc.cam.ac.uk/data_request/cif.

Acknowledgements

TKP gratefully acknowledges the Council of Scientific and Industrial Research (CSIR), India for the financial support (Project No. 01(2926)/18/EMR-II). SB thanks CSIR for research fellowships. RS acknowledges SERB (Project: YSS/2015/001741) for the Young Scientist Project.

Keywords: N-ligand • iron • benzilate • dioxygen • oxidation

[1] (a) R. P. Hausinger, *Crit. Rev. Biochem. Mol. Biol.* **2004**, *39*, 21-68; (b) M. Costas, M. P. Mehn, M. P. Jensen, L. Que, Jr., *Chem. Rev.* **2004**, *104*, 939-986; (c) T. D. H. Bugg, S. Ramaswamy, *Curr. Opin. Chem. Biol.* **2008**, *12*, 134-140; (d) P. C. A. Bruijnincx, G. van Koten, R. J. M. K. Gebbink, *Chem. Soc. Rev.* **2008**, *37*, 2716-2744; (e) E. G. Kovaleva, J. D. Lipscomb, *Nat. Chem. Biol.* **2008**, *4*, 186-193; (f) K. Ray, F. F. Pfaff, B. Wang, W. Nam, *J. Am. Chem. Soc.* **2014**, *136*, 13942-13958.

[2] (a) E. L. Hegg, L. Que, Jr., *Eur. J. Biochem.* **1997**, *250*, 625-629; (b) G. D. Straganz, B. Nidetzky, *ChemBioChem* **2006**, *7*, 1536-1548; (c) C. Loenarz, C. J. Schofield, *Nat. Chem. Biol.* **2008**, *4*, 152-156.

[3] S. Martinez, R. P. Hausinger, *J. Biol. Chem.* **2015**, *290*, 20702-20711.

[4] L. V. Liu, C. B. Bell, III, S. D. Wong, S. A. Wilson, Y. Kwak, M. S. Chow, J. Zhao, K. O. Hodgson, B. Hedman, E. I. Solomon, *Proc. Natl. Acad. Sci. U. S. A.* **2010**, *107*, 22419-22424, S22419/22411-S22419/22413.

[5] J. Rittle, M. T. Green, *Science* **2010**, *330*, 933-937.

[6] D. Galonić Fujimori, E. W. Barr, M. L. Matthews, G. M. Koch, J. R. Yonce, C. T. Walsh, J. M. Bollinger, Jr., C. Krebs, P. J. Riggs-Gelasco, *J. Am. Chem. Soc.* **2007**, *129*, 13408-13409.

[7] (a) J. C. Price, E. W. Barr, B. Tirupati, J. M. Bollinger, Jr., C. Krebs, *Biochemistry* **2003**, *42*, 7497-7508; (b) D. A. Proshlyakov, T. F. Henshaw, G. R. Monterosso, M. J. Ryle, R. P. Hausinger, *J. Am. Chem. Soc.* **2004**, *126*, 1022-1023.

[8] (a) M. L. Matthews, C. M. Krest, E. W. Barr, F. H. Vaillancourt, C. T. Walsh, M. T. Green, C. Krebs, J. M. Bollinger, Jr., *Biochemistry* **2009**, *48*, 4331-4343; (b) J. M. Bollinger, Jr., W.-c. Chang, M. L. Matthews, R. J. Martinie, A. K. Boal, C. Krebs, *RSC Metallobiol.* **2015**, *3*, 95-122.

[9] A. Karlsson, J. V. Parales, R. E. Parales, D. T. Gibson, H. Eklund, S. Ramaswamy, *Science* **2003**, *299*, 1039-1042.

[10] (a) S. Hong, Y.-M. Lee, W. Shin, S. Fukuzumi, W. Nam, *J. Am. Chem. Soc.* **2009**, *131*, 13910-13911; (b) A. Thibon, J. England, M. Martinho, V. G. Young, Jr., J. R. Frisch, R. Guillot, J.-J. Girerd, E. Münck, L. Que, Jr., F. Banse, *Angew. Chem. Int. Ed.* **2008**, *47*, 7064-7067.

[11] (a) F. Namuswe, T. Hayashi, Y. Jiang, G. D. Kasper, A. A. N. Sarjeant, P. Moënne-Loccoz, D. P. Goldberg, *J. Am. Chem. Soc.* **2010**, *132*, 157-167; (b) A. Franke, C. Fertinger, R. van Eldik, *Chemistry – A European Journal* **2012**, *18*, 6935-6949; (c) F. Namuswe, G. D. Kasper, A. A. N. Sarjeant, T. Hayashi, C. M. Krest, M. T. Green, P. Moënne-Loccoz, D. P. Goldberg, *J. Am. Cherm. Soc.* **2008**, *130*, 14189-14200; (d) N. Lehnert, R. Y. N. Ho, L. Que, Jr., E. I. Solomon, *J. Am. Chem. Soc.* **2001**, *123*, 8271-8290.

[12] (a) W. Nam, *Acc. Chem. Res.* **2015**, *48*, 2415-2423; (b) L. Que, Jr., *Acc. Chem. Res.* **2007**, *40*, 493-500; (c) A. R. McDonald, L. Que, Jr., *Coord. Chem. Rev.* **2013**, *257*, 414-428; (d) W. Nam, Y.-M. Lee, S. Fukuzumi, *Acc. Chem. Res.* **2014**, *47*, 1146-1154; (e) X. Engelmann, I. M.-Pérez, K. Ray, *Angew. Chem. Int. Ed.* **2016**, *55*, 7632-7649; (f) J. England, M. Martinho, E. R. Farquhar, J. R. Frisch, E. L. Bominaar, E. Münck, L. Que, *Angew. Chem. Int. Ed.* **2009**, *48*, 3622-3626; (g) A. N. Biswas, M. Puri, K. K. Meier, W. N. Oloo, G. T. Rohde, E. L. Bominaar, E. Münck, L. Que, Jr., *J. Am. Chem. Soc.* **2015**, *137*, 2428-2431; (h) M. Puri, L. Que, Jr., *Acc. Chem. Res.* **2015**, *48*, 2443-2452; (i) S. H. Bae, M. S. Seo, Y.-M. Lee, K.-B. Cho, W.-S. Kim, W. Nam, *Angew. Chem., Int. Ed.* **2016**, *55*, 8027-8031.

[13] (a) H. Hirao, D. Kumar, L. Que, Jr., S. Shaik, *J. Am. Chem. Soc.* **2006**, *128*, 8590-8606; (b)E. J. Klinker, S. Shaik, H. Hirao, L. Que, Jr., *Angew. Chem. Int. Ed.* **2009**, *48*, 1291-1295.

[14] (a) S. Sahu, L. R. Widger, M. G. Quesne, S. P. de Visser, H. Matsumura, P. Moënne-Loccoz, M. A. Siegler, D. P. Goldberg, *J. Am.*

Chem. Soc. **2013**, *135*, 10590-10593; (b) M. Mitra, H. Nimir, S. Demeshko, S. S. Bhat, S. O. Malinkin, M. Haukka, J. Lloret-Fillol, G. C. Lisensky, F. Meyer, A. A. Shteinman, W. R. Browne, D. A. Hrovat, M. G. Richmond, M. Costas, E. Nordlander, *Inorg. Chem.* **2015**, *54*, 7152-7164; (c) I. Monte Perez, X. Engelmann, Y.-M. Lee, M. Yoo, E. Kumaran, E. R. Farquhar, E. Bill, J. England, W. Nam, M. Swart, K. Ray, *Angew. Chem., Int. Ed.* **2017**, *56*, 14384-14388; (d) W. Rasheed, A. Draksharapu, S. Banerjee, V. G. Young, Jr., R. Fan, Y. Guo, M. Ozerov, J. Nehrkorn, J. Krzystek, J. Telser, L. Que, Jr., *Angew. Chem., Int. Ed.* **2018**, *57*, 9387-9391; (e) Y. Zang, J. Kim, Y. Dong, E. C. Wilkinson, E. H. Appelman, L. Que, Jr., *J. Am. Chem. Soc.* **1997**, *119*, 4197-4205.

[15] R. Singh, G. Ganguly, S. O. Malinkin, S. Demeshko, F. Meyer, E. Nordlander, T. K. Paine, *Inorg. Chem.* **2019**, *58*, 1862-1876.

[16] B. Chakraborty, R. D. Jana, R. Singh, S. Paria, T. K. Paine, *Inorg. Chem.* **2017**, *56*, 359-371.

[17] M. Lubben, R. Hage, A. Meetsma, K. Bÿma, B. L. Feringa, *Inorg. Chem.* **1995**, *34*, 2217-2224.

[18] S. Chatterjee, D. Sheet, T. K. Paine, *Chem. Commun.* **2013**, *49*, 10251-10253.

[19] (a) Y.-M. Chiou, L. J. Que, *J. Am. Chem. Soc.* **1995**, *117*, 3999-4013; (b) S. Ménage, Y. Zang, M. P. Hendrich, L. Que, Jr., *J. Am. Chem. Soc.* **1992**, *114*, 7786-7792; (c) G. J. P. Britovsek, J. England, A. J. P. White, *Inorg. Chem.* **2005**, *44*, 8125-8134.

[20] (a) S. Paria, L. Que, Jr., T. K. Paine, *Angew. Chem. Int. Ed.* **2011**, *50*, 11129-11132; (b) S. Paria, S. Chatterjee, T. K. Paine, *Inorg. Chem.* **2014**, *53*, 2810-2821.

[21] S. Chatterjee, T. K. Paine, *Angew. Chem. Int. Ed.* **2015**, *54*, 9338-9342.

[22] S. Chatterjee, S. Bhattacharya, T. K. Paine, *Inorg. Chem.* **2018**, *57*, 10160-10169.

[23] S. Chatterjee, T. K. Paine, *Angew. Chem. Int. Ed.* **2016**, *55*, 7717-7722.

[24] W. C. Wolsey, *J. Chem. Educ.* **1973**, *50*, A335-A337.

[25] Bruker, Bruker AXS, Madison, WI, **2006**.

[26] G. M. Sheldrick, *SHELXL-97, Program for crystal structure refinement*, University of Göttingen, Göttingen, Germany, **1997**.

10.1002/asia.202000142

Entry for the Table of Contents

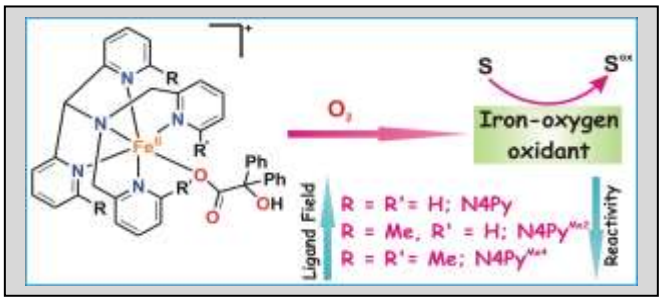

Playing with Ligand Field: The oxidizing ability of iron(II)-benzilate complexes of pentadentate nitrogen donor ligands is greatly influenced by electronic and structural tuning of the supporting ligand. With decreasing ligand fields, the reactivity of dioxygen-derived iron-oxygen oxidants increases in oxygen-and hydrogen-atom transfer reactions towards organic substrates.